



Formation and Coloring Mechanism of Typical Aluminosilicate Clay Minerals for CoAl_2O_4 Hybrid Pigment Preparation

Anjie Zhang^{1,2,3}, Bin Mu^{1*}, Xiaowen Wang^{1,2}, Lixin Wen³ and Aiqin Wang^{1*}

¹ Key Laboratory of Clay Mineral Applied Research of Gansu Province, Center of Eco-material and Green Chemistry, Lanzhou Institute of Chemical Physics, Chinese Academy of Sciences, Lanzhou, China, ² University of Chinese Academy of Sciences, Beijing, China, ³ Northwest Yongxin Coatings Limited Company, Lanzhou, China

OPEN ACCESS

Edited by:

Pu-Xian Gao,
University of Connecticut,
United States

Reviewed by:

Sibo Wang,
University of Connecticut,
United States
Kaixuan Bu,
Rutgers University, The State
University of New Jersey,
United States
Quansheng Liu,
Changchun University of Technology,
China

*Correspondence:

Bin Mu
mubin@licp.cas.cn
Aiqin Wang
aqwang@licp.cas.cn

Specialty section:

This article was submitted to
Green and Sustainable Chemistry,
a section of the journal
Frontiers in Chemistry

Received: 05 February 2018

Accepted: 03 April 2018

Published: 19 April 2018

Citation:

Zhang A, Mu B, Wang X, Wen L and
Wang A (2018) Formation and
Coloring Mechanism of Typical
Aluminosilicate Clay Minerals for
 CoAl_2O_4 Hybrid Pigment Preparation.
Front. Chem. 6:125.
doi: 10.3389/fchem.2018.00125

Different kinds of aluminosilicate minerals were employed to fabricate CoAl_2O_4 hybrid pigment for studying its formation and coloring mechanism. It revealed that the color of the obtained hybrid pigments was determined by the content of Al_2O_3 and lightness of clay minerals. The higher the Al_2O_3 content and the lightness of clay minerals, the better the color parameters of hybrid pigments. During the preparation of hybrid pigments, CoAl_2O_4 nanoparticles were confined to be loaded on the surface of the aluminosilicate minerals, which effectively prevented from the aggregation and the size increase of CoAl_2O_4 nanoparticles. What's more, aluminosilicate mineral might be an ideal natural aluminum source to compensate the aluminum loss due to the dissolution of $\text{Al}(\text{OH})_3$ at alkaline medium during precursor preparation, keeping an optimum molar ratio of $\text{Co}^{2+}/\text{Al}^{3+}$ for formation of spinel CoAl_2O_4 pigments in the process of high-temperature crystallization.

Keywords: CoAl_2O_4 , aluminosilicate minerals, hybrid pigments, formation mechanism, coloring mechanism

INTRODUCTION

AB_2O_4 spinel complex oxides usually are used as ceramic materials, inorganic pigments, magnetic materials, catalysts and gas-sensitive materials (Ren et al., 2014; Yoneda et al., 2016; Zou and Zheng, 2016; Álvarez-Docio et al., 2017; Chafi et al., 2017; Rani, 2017; Tang et al., 2017), the most famous one of them is cobalt aluminate (CoAl_2O_4). As a high-grade eco-friendly intense blue pigment, it can be applied in the fields of ceramics, plastics, paint, glass, and color TV tubes due to high refractive index, excellent chemical, and thermal stability (Mahé et al., 2008; Ryu et al., 2008; Tirsoaga et al., 2011; Merino et al., 2015; Soleimani-Gorgania et al., 2015). However, the high cost of CoAl_2O_4 pigments has severely restrained their wide applications because of the expensive cobalt compounds (De Souza et al., 2009; Gholizadeh and Malekzadeh, 2017; Zhang et al., 2017). In addition, the traditional method for preparation of cobalt blue pigment was involved in the calcination of CoO and Al_2O_3 at above $1,300^\circ\text{C}$ for a long time (Armijo, 1969; Salavati-Niasari et al., 2009; Sale, 2015; He et al., 2017; Zhang et al., 2017), which was obviously time-consuming. Therefore, it is urgent to develop a strategy to prepare the low-cost cobalt blue pigment with perfect color property in order to realize its wide applications.

Incorporation of non-toxic and low-cost elements may be an efficient method to decrease the use of Co element. Torkian et al. synthesized $\text{Co}_x\text{Mg}_{1-x}\text{Al}_2\text{O}_4$ nanopigment based on the substitution

of Co²⁺ using Mg²⁺ via combustion method (Torkian et al., 2013). Khattab et al. also synthesized Co_xMg_{1-x}Al₂O₄ blue pigment after replacing of Co²⁺ with Mg²⁺ during the calcination process (Khattab et al., 2017), and Sedghi prepared Co_xZn_{1-x}Al₂O₄ nano-pigments by gel combustion method (Sedghi et al., 2014). It suggests that the doping technology using the matched metal ions can enhance the color properties as well as decrease the cost of cobalt blue. However, the decrease in the cost of cobalt blue is limited by the substitution of Co²⁺ using other metal ions. What's more, the agglomeration and crystal grain growth of cobalt blue nanoparticles still remain during calcining process.

Recently, many inorganic substrates are employed to construct the eco-friendly high-grade inorganic hybrid pigment (Mousavand et al., 2006; Zhang et al., 2015; Meng et al., 2016; Mishra et al., 2017; Tian et al., 2017). Due to the abundance in nature, low-cost, non-toxic and unique structure features, clay minerals can be served as a promising substrate for loading of the inorganic nanoparticles (Wang et al., 2011; Todorova et al., 2014; Mu and Wang, 2015; Ezzatahmedi et al., 2017; Intachai et al., 2017). Therefore, our groups have prepared cobalt blue hybrid pigments after incorporating of attapulgite, halloysite (Hal), montmorillonite (Mt), etc., via co-precipitation method followed by a calcination process (Mu et al., 2015; Zhang et al., 2017). It has confirmed that the introduction of clay minerals dramatically decreases the cost of pigment, as well as improves the aggregation of cobalt blue nanoparticles. In addition, some components of clay minerals might enter into tetrahedral or octahedral positions of CoAl₂O₄ spinel structure to substitute Co²⁺ or Al³⁺, which have an obvious effect on the color properties of cobalt blue. However, the relevant formation and coloring mechanism of the CoAl₂O₄/clay mineral hybrid pigments was still not clear. Therefore, several of typical aluminosilicate minerals were selected to construct the CoAl₂O₄/aluminosilicate clay mineral hybrid pigments to study its relevant formation and coloring mechanism in this study, the involved clay minerals included Hal, Mt, kaoline (Kaol), andalusite (And), dickite (Dic), mullite (M47 and M70, the number is indicator of the Al₂O₃ content). The effect of the different aluminosilicate clay minerals on the color parameters of hybrid pigment was studied in detail, and the possible formation and coloring mechanism of the hybrid pigments was proposed. It is expected to provide guidance for preparation of low-cost and high-grade cobalt blue with the perfect color properties.

EXPERIMENTAL

Materials

Hal and And were obtained from Zhengzhou Jinyanguang Ceramics Co., Ltd. (HeNan, China). Mt, Dic, M47 and M70 were obtained from Yixian Kaolin Development Co., Ltd. (HeBei, China), Qingdao Yuzhou chemical Co., Ltd. (ShanDong, China), Huakang Non-Metallic Minerals Processing Plants (HeBei, China), respectively. Kaol was purchased from Longyan Kaolin Co., Ltd. (FuJian, China). In order to analyze the compositions of aluminosilicate minerals using X-ray fluorescence, the

aluminosilicate minerals were firstly crushed and purified by 4% HCl (wt%) to remove carbonates, and then the purified clay minerals were filtered by passing through a 200-mesh sieve. The composition of the involved aluminosilicate minerals is summarized in **Table 1**. Co(NO₃)₂·6H₂O and Al(NO₃)₃·9H₂O were purchased from Shanghai Reagent Factory (Shanghai, China). NaOH, HCl, and anhydrous ethanol were obtained by China National Medicines Co., Ltd.

Preparation of CoAl₂O₄/Aluminosilicate Clay Mineral Hybrid Pigment

The CoAl₂O₄/aluminosilicate clay mineral hybrid pigments were fabricated according to the similar procedure reported in our previous study (Zhang et al., 2017). Co(NO₃)₂·6H₂O (0.01 mol), Al(NO₃)₃·9H₂O (0.02 mol), and 1.090 g of aluminosilicate clay mineral (60 wt% of CoAl₂O₄) were added into water (50 mL) and magnetically stirred at 150 rpm for 1 h. And then the pH value of the reaction system was adjusted to 10 using 3 M NaOH aqueous solution and stirred for 2 h at room temperature. The obtained solid products were collected by centrifugation, and washed more than five times using water before being dried at 60°C for 10 h. Finally, it was calcined at 1,100°C for 2 h with a rate of 10°C/min from room temperature to 1,100°C, and the as-prepared hybrid pigments were abbreviated to Kaol-HP, Hal-HP, Mt-HP, M47-HP, M70-HP, And-HP, and Dic-HP corresponding to different clay minerals, respectively. As a control, cobalt blue pigments without clay minerals also were fabricated by the same procedures, and the productions were labeled to CoAl₂O₄-900, CoAl₂O₄-1000, CoAl₂O₄-1100, and CoAl₂O₄-1200 according to the calcining temperatures, respectively. In additional, different clay minerals were also calcined at 1,100°C and defined as Kaol-1100, Hal-1100, Mt-1100, M47-1100, M70-1100 And-1100, and Dic-1100, respectively.

Characterization

The morphology was measured using transmission electron microscopy (TEM, JEM-1200EX/S, JEOL). The structure and composition was analyzed using Fourier Transform infrared (FTIR, Thermo Nicolet NEXUS TM, Madison, USA). The X'pert PRO diffractometer ($\lambda = 1.54060\text{\AA}$) was used to analysis the XRD patterns of the sample with a scan step size of 0.02° per second. Raman spectra were recorded using the microprobe on a

TABLE 1 | Chemical composition of different clay minerals after acid treatment.

Clay minerals	Al ₂ O ₃ (%)	Na ₂ O (%)	MgO (%)	CaO (%)	SiO ₂ (%)	K ₂ O (%)	Fe ₂ O ₃ (%)	TiO ₂ (%)
Hal	29.49	0	0.39	0.08	41.15	0.61	1.71	–
Kaol	54.2	0.014	0.45	0.32	23.5	3.3	0.67	1.36
Mt	22	–	–	–	64.6	5.24	6.03	1.34
Dic	26.2	–	–	0.24	54.1	0.49	0.26	–
And	56.5	–	–	0.37	38.7	1.18	1.39	1.38
M47	49.1	–	–	0.92	42.8	0.96	2.38	3.07
M70	64.6	–	–	0.99	25.5	1.17	2.1	1.02

Labram HR Evolution Raman spectrometer (Horiba). The Color-Eye automatic differential colorimeter (X-Rite, Ci 7800) was used to study the color properties of the as-prepared pigments by the Commission Internationale de l'Éclairage (CIE) 1976 L^* , a^* , b^* colorimetric method. L^* is the lightness axis (0 for black and 100 for white). The parameters of a^* (negative values for green and positive values for red) and b^* (negative values for blue and positive values for yellow) denote the hue or color dimensions.

RESULTS AND DISCUSSION

Characterization of Kaol-HP

Figure S1 (see ESI) gives the CIE parameters of Kaol-HP calcined at different temperatures. It is observed that the L^* value of hybrid pigments firstly increases with the increase of the calcining temperatures, and then it decreases as the temperature is above 1,100°C. The same change trend is also observed from the value of b^* of Kaol-HP, but the color of CoAl₂O₄ pigments without Kaol is different compared with that of Kaol-HP prepared under the same conditions. In order to obtain the blue color, the calcining temperature for preparation of CoAl₂O₄ pigments without Kaol must be above 1,200°C (Figure S2, see ESI), but its color properties ($L^* = 37.41$, $a^* = -0.52$, $b^* = -41.14$) are poor compared with Kaol-HP prepared at 1,100°C ($L^* = 48.11$, $a^* = 2.64$, $b^* = -63.75$). Thus these two samples are selected to investigate the effect of introduction of clay minerals on the structure and properties of pigments. However, the L^* value of Kaol-HP decreases when the temperature increases to 1,200°C, which might be due to the crystal phase transition and the collapse of Kaol structure (Juneja et al., 2010; Yeo, 2011; Zhang et al., 2017).

Figure 1A presents the FTIR spectra of the raw Kaol, Kaol calcined at 1,100°C, Kaol-HP, and CoAl₂O₄ calcined at 1,200°C. As depicted in the FTIR spectrum of the raw Kaol, the band at 3,684 and 3,651 cm⁻¹ are assigned to stretching vibrations of Al-OH (Saikia and Parthasarathy, 2010). The bands at 3,440 and 1,636 cm⁻¹ are assigned to the physisorbed water on the surface of Kaol and the bending vibration of H-O-H, respectively. The IR peaks at 911 cm⁻¹ can be ascribed to the Al-Al-OH vibration of the clay sheet, while the bands located at 1,114, 1,096, 1,032, and 471 cm⁻¹ are related to Si-O-Si of the clay tetrahedron sheets (Jafari and Hassanzadeh-Tabrizi, 2014). After being calcined at 1,100°C, the typical absorption bands of Kaol at 3,651, 3,684, and 911 cm⁻¹ disappear due to the dehydroxylation of Kaol during calcination. After incorporating of CoAl₂O₄ nanoparticles, the characteristic absorption bands of CoAl₂O₄ at 668, 557, and 509 cm⁻¹ were clearly observed, which correspond to the stretching vibration of Al-O of AlO₆ and Co-O of CoO₄ (Chapskaya et al., 2005), respectively. Furthermore, these characteristic adsorption bands also can be found in the FTIR spectrum of CoAl₂O₄ pigments.

Figure 1B exhibits the XRD patterns of the raw Kaol, Kaol calcined at 1,100°C, Kaol-HP, and CoAl₂O₄ calcined at 1,200°C. The raw Kaol presents well-defined reflections at $2\theta = 12$ and 25° , which are typical characteristic peaks of kaolinite (Panda et al., 2010; Konduri and Fatehi, 2017). The diffraction peak

of mica is observed at $2\theta = 8.9^\circ$ while the ones located at $2\theta = 18.3$ and 20.2° are attributed to the diffraction peaks of Hal. It indicates that the raw Kaol is associated with Hal, quartz and mica. When Kaol is calcined at 1,100°C, the typical diffraction peaks of Kaol, Hal, and mica disappear, and only the diffraction peaks of quartz remain. As for Kaol-HP, it is obvious that the typical diffraction peaks of Kaol vanish accompanied with the presence of some new diffraction peaks, which are assigned to spinel CoAl₂O₄. According to JCPD card No. 10-458, the diffraction peaks located at $2\theta = 31.1, 36.8, 44.8, 49.0, 55.5, 59.2, 65.2^\circ$ correspond to (220), (311), (400), (331), (422), (511), and (440) of CoAl₂O₄, respectively (Abaide et al., 2015). In order to study the effect of calcining temperatures and incorporating of clay minerals on the sizes of CoAl₂O₄, the crystallite size is also calculated using Sherrer relation according to XRD patterns of all samples (including hybrid pigments prepared using Kaol at different temperatures, see Figure S3) (Equation 1):

$$D = \frac{0.89 \times \lambda}{B \times \cos \theta} \quad (1)$$

where D is the crystallite size, λ is the wavelength (Cu Ka), θ is the diffraction angle of the most intense diffraction peak (Zhang et al., 2018), B is the corrected half-width obtained using a quartz as reference. $B = B_m - B_s$, where B_m refers to the tested results and B_s was got by testing a reference substance. As shown in Table S1, it is clear that the crystallite sizes of CoAl₂O₄ increases with the increase of the calcining temperatures either hybrid pigments or CoAl₂O₄ pigments without Kaol. However, the crystallite sizes of the as-prepared hybrid pigments are smaller than that of CoAl₂O₄ pigments, suggesting that the introduction of clay minerals obviously prevents from the increase in size and the agglomeration of CoAl₂O₄ particles during calcining process.

Figure 2a provides the TEM image of Kaol, and it can be found that Kaol is a typical lamellar layered structure with a smooth surface, and some tubular morphology is also observed, which can be attributed to the associated tubular Hal. The length of Hal is around 0.2–2.0 μm while the external and inner diameters are about 50–80 and 20–50 nm, respectively. After being calcined at 1,100°C (**Figure 2b**), the lamellar morphology of Kaol remains while the tubular structure is transformed into rodlike one, which is possible related to the phase transformation of Hal. After introducing of CoAl₂O₄ nanoparticles, the surface of lamellar morphology becomes coarse due to the loading of CoAl₂O₄ nanoparticles. The CoAl₂O₄ nanoparticles with a diameter of about 10–20 nm are uniformly anchored on the surface of lamellar (**Figure 2c**). Furthermore, the selected area electron diffraction pattern of Kaol-HP calcined at 1,100°C also confirmed the formation of CoAl₂O₄ nanoparticles (Figure S4, see ESI) (Ouahdi et al., 2005; Mindru et al., 2010). In addition, **Figure 2d** gives an enlarged electron micrograph of **Figure 2c**, it provides a well-resolved lattice plane with an interplanar spacing of 0.244 nm, corresponding to [311] plane of the cubic $Fd\bar{3}m$ space group, which is identified on the basis of data from the standard CoAl₂O₄ database JCPD card no. 10-458 (Kim et al., 2012). The micrograph displays the coexistence of amorphous and crystalline phases, and the crystalline phase

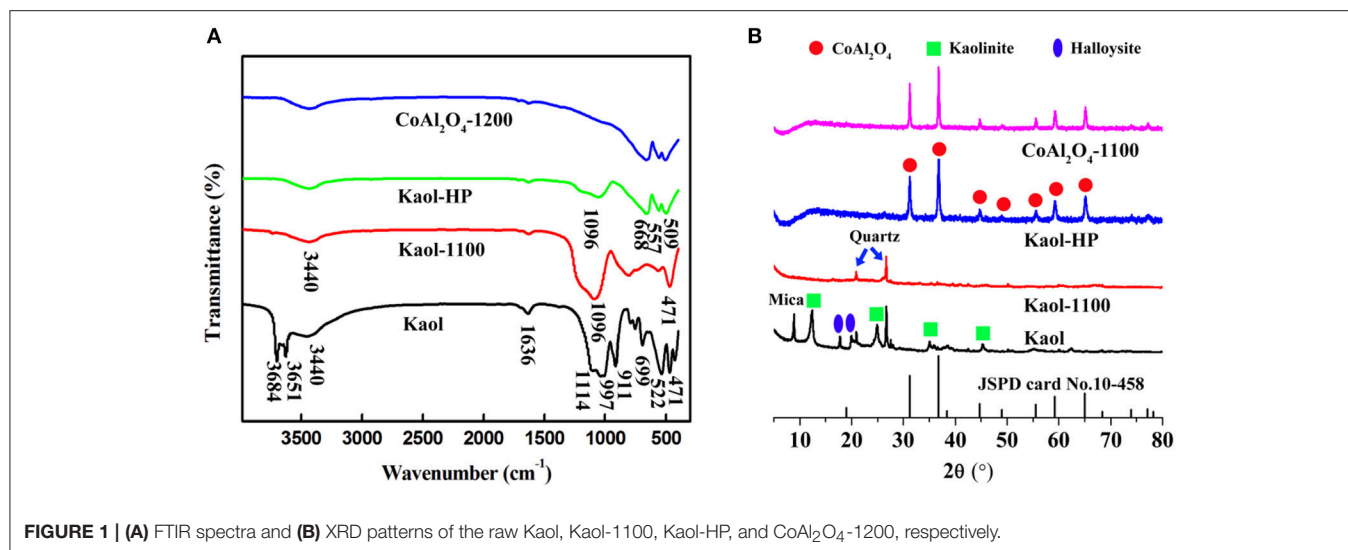


FIGURE 1 | (A) FTIR spectra and **(B)** XRD patterns of the raw Kaol, Kaol-1100, Kaol-HP, and CoAl₂O₄-1200, respectively.

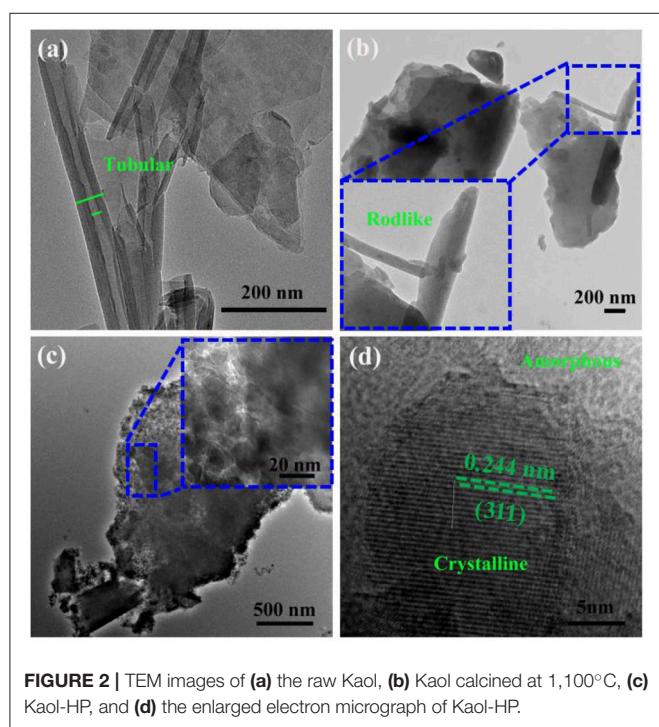


FIGURE 2 | TEM images of **(a)** the raw Kaol, **(b)** Kaol calcined at 1,100°C, **(c)** Kaol-HP, and **(d)** the enlarged electron micrograph of Kaol-HP.

might be attributed to the spinel CoAl₂O₄ while the amorphous one is related to silicate derived from Kaol (Cho and Kakihana, 1999).

Figure S5 depicts the EDX spectrum of Kaol-HP, and it can be found that Kaol-HP is mainly composed of Co, Al, O, and Si elements. Element mapping of Kaol-HP is illustrated in **Figure 3**, it is clear that Co element is uniformly distributed on the surface of lamellar, suggesting that the generated CoAl₂O₄ is well anchored on the surface of substrate. Furthermore, other elements also present the uniform distribution. By contrast, the edge color of Si element is obscure, which can be attributed to

the fact that the edge thickness of the silicate substrate is thin. However, the value of Co/Al decreases from 0.49 to 0.37 to 0.31 with the change of the selected area from boundary to center of Kaol-HP (**Table 2**), which indicates the loading content of CoAl₂O₄ in the edge reign is higher than the center of the silicate substrate. Based on the above analysis, it suggests that Kaol-HP has been successfully prepared.

Effect of Different Aluminosilicate Clay Minerals and Coloring Mechanism

In our previous study (Zhang et al., 2017), it has been confirmed that the introduction of clay minerals, especially aluminosilicate mineral of Hal, was in favor of decreasing the formation temperature of spinel-type CoAl₂O₄, and enhancing the color properties of CoAl₂O₄ pigment. In order to investigate the effect of the different aluminosilicate minerals on the color properties of hybrid pigments, several of representative aluminosilicate minerals were selected to prepare CoAl₂O₄ hybrid pigments including Hal, And, Kaol, Mt, Dic, M47, and M70.

The XRD patterns of the different aluminosilicate minerals are provided in **Figure 4**. Hal is a 1:1 aluminosilicate mineral with the empirical formula Al₂Si₂O₅(OH)₄, the typical diffraction peaks of Hal are observed at $2\theta = 12.3, 18.3, 20.2, 24.8^\circ$, and the diffraction peaks of quartz are located at $2\theta = 20.8, 26.7,$ and 36.6° (**Figure 4A**) (Philip et al., 2017). **Figure 4B** gives XRD pattern of Mt, its characteristic diffraction peaks are located at $2\theta = 5.9, 19.7,$ and 35.1° , while the diffraction peaks at $2\theta = 12.5$ and 17.5° are attributed to illite (Wang et al., 2016; Liang et al., 2017). Dic is a kind of layered silicate mineral, and pertains to 1:1 type of Kaol subgroup. As shown in **Figure 4C**, the characteristic diffraction peaks between 34 and 39° can be observed, which are assigned to (200), (131), (006), and (133) of Dic, respectively (Zheng et al., 2011). **Figures 4D–F** depicted the XRD patterns of M47, M70, and And. Mullite is an artificial material, which is synthesized using natural raw materials during 1,100–1,600°C, such as And, kyanite, etc. (Xu et al., 2017; Yuan et al., 2017).

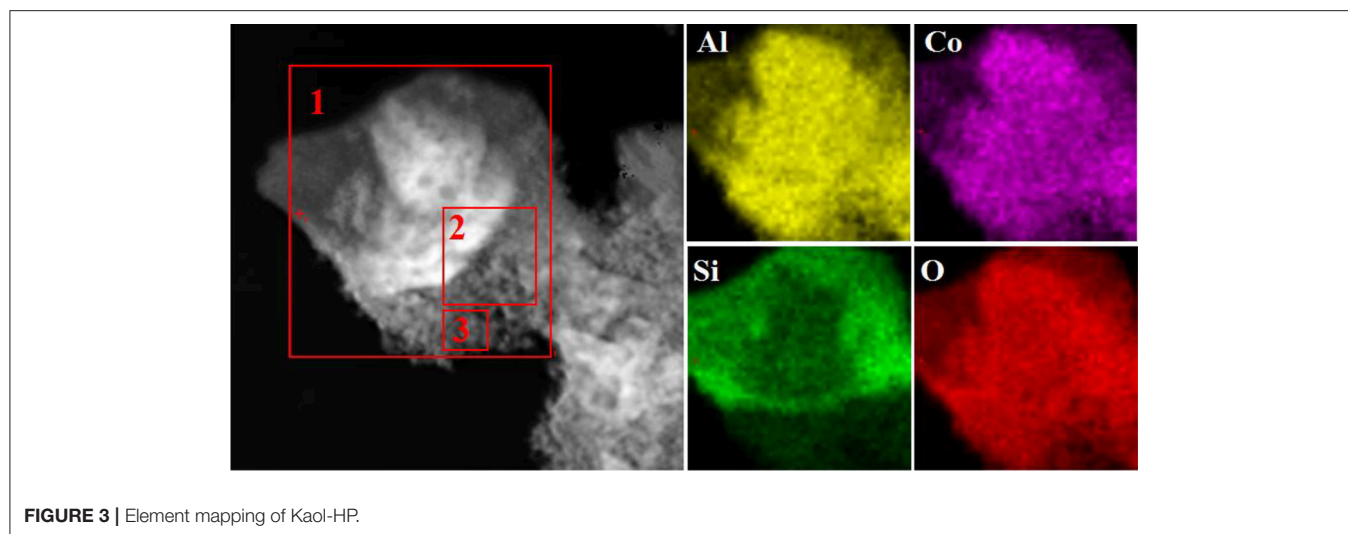


FIGURE 3 | Element mapping of Kaol-HP.

TABLE 2 | The element content of the different selection areas of Kaol-HP.

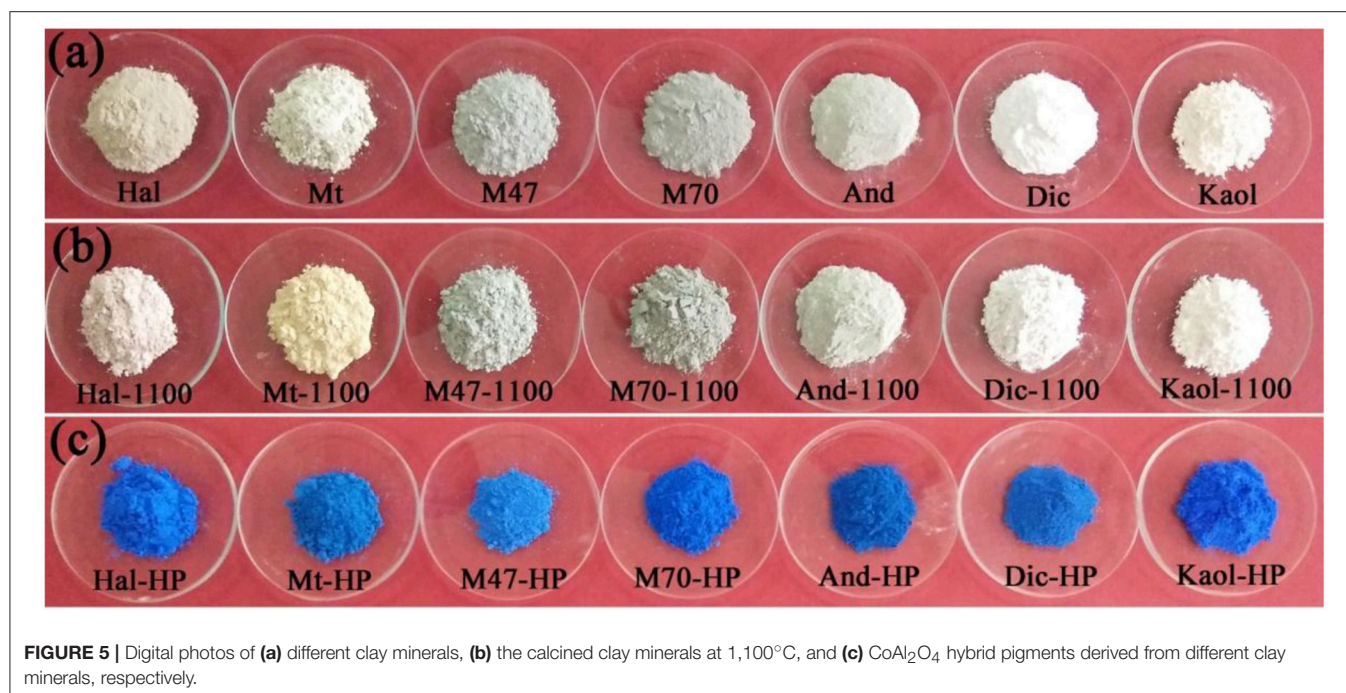
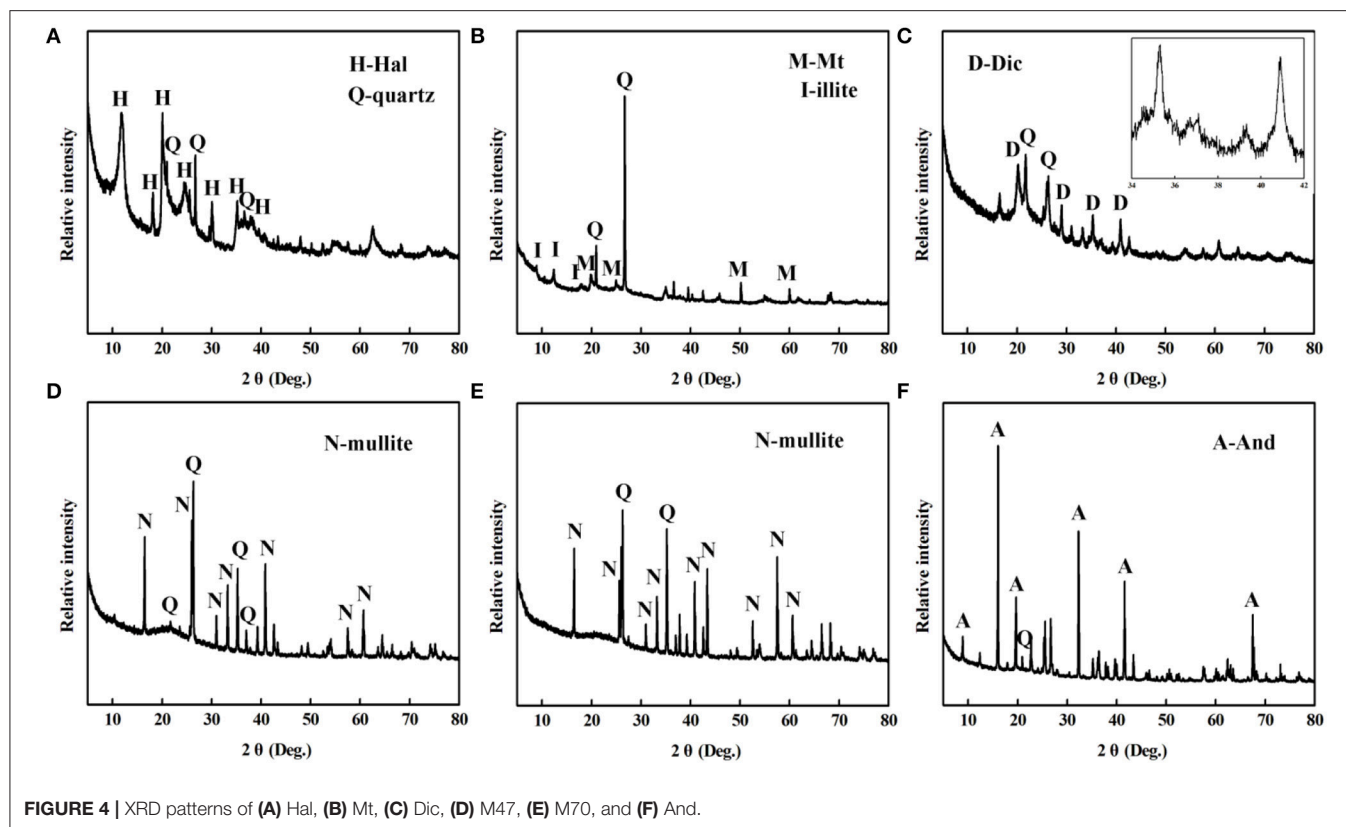
Element	Atomic (%)		
	No. 1	No. 2	No. 3
O	67	63.61	51.21
Na	0.95	0.90	0.47
Al	17.01	21.06	31.55
Si	9.49	6.17	1.35
K	0.35	0.22	0
Co	5.18	8.01	15.39
Co/Al	0.31	0.37	0.49
Total	100	100	100

Figure 5 shows the digital photos of the raw aluminosilicate clay minerals, the calcined aluminosilicate clay minerals at 1,100°C and CoAl₂O₄ hybrid pigments derived from different aluminosilicate clay minerals, respectively. It is obvious that different clay minerals present different colors. Dic and Kaol are white, Hal and Mt are light brown, while M47, M70, and And are gray. After being calcined at 1,100°C (Figure 5b), Kaol and Dic are white, Mt is yellowish-brown, Hal was light pink, and the others (M47, M70, and And) are gray. The digital photos of the as-prepared hybrid pigments are exhibited in Figure 5c, it is found that all hybrid pigments present typical blue, but there are differences among different hybrid pigments. By contrast, the color of Kaol-HP is optimal, which is also consistent with their color parameters (Table 3). Kaol-HP exhibits the maximum b^* and C^* values, followed by M70-HP, M47-HP, Hal-HP, respectively, while Mt-HP and And-HP indicate the worst lightness (L^*). It suggests that the colors of the hybrid pigments might be related to the types and compositions of aluminosilicate clay minerals.

As shown in Table 1, the main compositions of the involved aluminosilicate clay minerals are Al₂O₃ and SiO₂. Therefore, the relationship between the content of Al₂O₃ or SiO₂ and the color

parameters of hybrid pigments are investigated, and Figure 6 gives the relationship between the CIE parameters of CoAl₂O₄ hybrid pigments and the content of Al₂O₃ and SiO₂ of different aluminosilicate clay minerals, while Table S2 summarizes the content of Al₂O₃ and SiO₂ of the clay minerals and the CIE of hybrid pigments. As a whole, the value of a^* of hybrid pigments increases with the increase in the content of Al₂O₃, but the b^* value becomes more negative. It indicates the blue color of hybrid pigments become deeper with the increase in the Al₂O₃ content. However, the b^* value is more positive with the increase in the content of SiO₂, indicating a poor blue color. Therefore, Al₂O₃ and SiO₂ of aluminosilicate clay minerals plays an important role in adjusting the color of CoAl₂O₄ hybrid pigments, but the ultimate color properties of hybrid pigments result from the synergy of various compositions of aluminosilicate clay minerals, besides their colors. In order to prove above proposal, Al₂O₃ and SiO₂ with different added amounts were employed to fabricate hybrid pigments without clay minerals, respectively. As shown in Figure 7, the b^* value of hybrid pigments prepared using Al₂O₃ gradually decreases with the increase in the added amounts of Al₂O₃ (more negative). On the contrary, the b^* value of hybrid pigments derived from SiO₂ increases with the increase in the amount of SiO₂ (more positive), which might be attributed to the formation of cobalt silicate (Llusar et al., 2001). This variation trend is also in agreement with the results of Figures 6A,B.

In addition, the pH value of the reaction system is crucial to cobalt-aluminum double hydroxides (Co/Al DH) (Zhang et al., 2017), the excess OH⁻ affects the molar ratio of Co/Al in the ultimate CoAl₂O₄ due to the dissolution loss of Al in alkaline medium, which directly determines the color properties of pigments. In order to prove this effect, HCl was added into the centrifugate after the co-precipitation reaction, it can clearly observe the white precipitate upon the addition of HCl (1.0 M), and the precipitate is confirmed to be Al(OH)₃ using FTIR technique (Figure S6, see ESI) (Kamaraj and Vasudevan, 2016). In addition, the higher the pH values of the reaction, the more



the contents of white precipitate (Figure S6, see ESI). When the pH value of reaction system is above 10, the generated Al(OH)₃ will partially dissolve and the molar ratio of Co²⁺/Al³⁺ is <2,

which can be confirmed by the EDX of CoAl₂O₄ in the absence of clay minerals during preparation. As shown in Figure S7, the value of Co/Al of CoAl₂O₄ in the absence of clay minerals

is about 0.62, and thus the Al loss is about 20% due to the dissolution of Al(OH)₃ at alkaline medium during preparation of precursor. Therefore, the incorporation of aluminosilicate clay

mineral may be an ideal natural aluminum sources to compensate the aluminum loss due to the dissolution of Al(OH)₃ at alkaline medium during preparation of precursor, keeping an optimum molar ratio of Co²⁺/Al³⁺ for formation of spinel CoAl₂O₄ pigment. It can be inferred that the Al originated from clay minerals about 20% might be participated in reaction and enter into the octahedral positions of CoAl₂O₄ spinel structure to form CoAl₂O₄-silicate solid solution (Tang et al., 2018). This is also can be confirmed by the production derived from Co²⁺ salt and Kaol in the absence of Al³⁺ salt, which is prepared using the same procedure with Kaol-HP. As shown in Figure S8, the XRD pattern of the product presents the characteristic diffraction peaks of CoAl₂O₄ suggesting that Kaol can be served as an aluminum source to form CoAl₂O₄. The evolution process might be depicted by the following process (Figure 8) (Zhong et al., 1999; Cava et al., 2006).

TABLE 3 | CIE parameters of the different CoAl₂O₄ hybrid pigment.

Hybrid pigments	L*	a*	b*	C*
Hal-HP	54.60	-4.30	-50.10	50.28
Kaol-HP	48.11	2.64	-63.75	63.80
Mt-HP	29.66	-13.97	-43.33	45.53
Dic-HP	49.14	-8.27	-47.63	48.34
And-HP	30.26	-10.41	-54.69	55.67
M47-HP	40.69	-14.65	-52.43	54.44
M70-HP	33.53	-1.63	-58.45	58.47

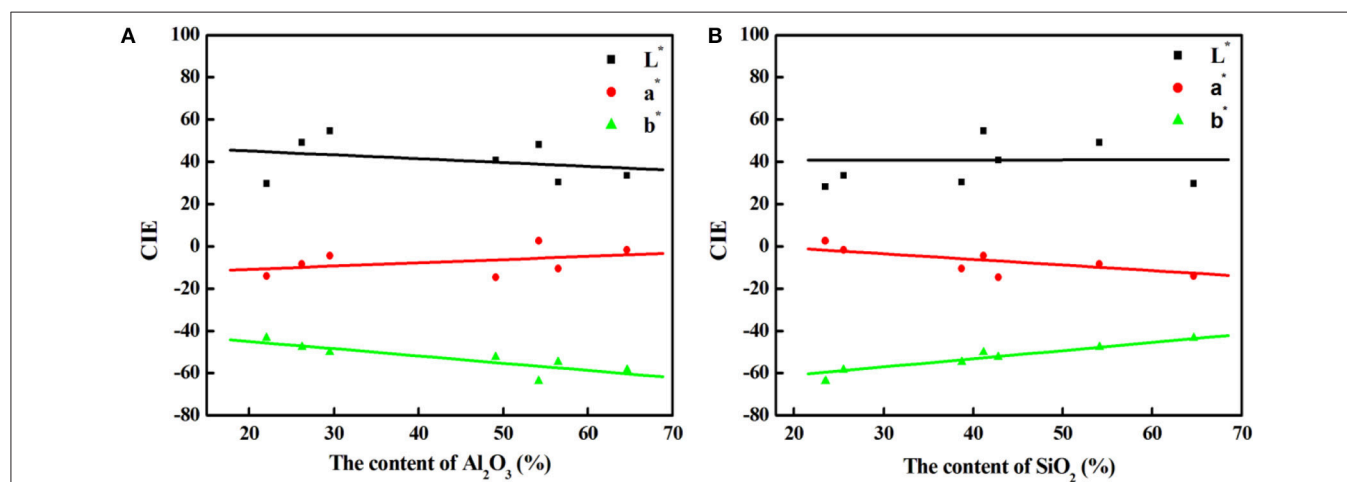


FIGURE 6 | The relationship between the CIE parameters of CoAl₂O₄ hybrid pigments and the content of Al₂O₃ (A) and SiO₂ (B) of different clay minerals, respectively.

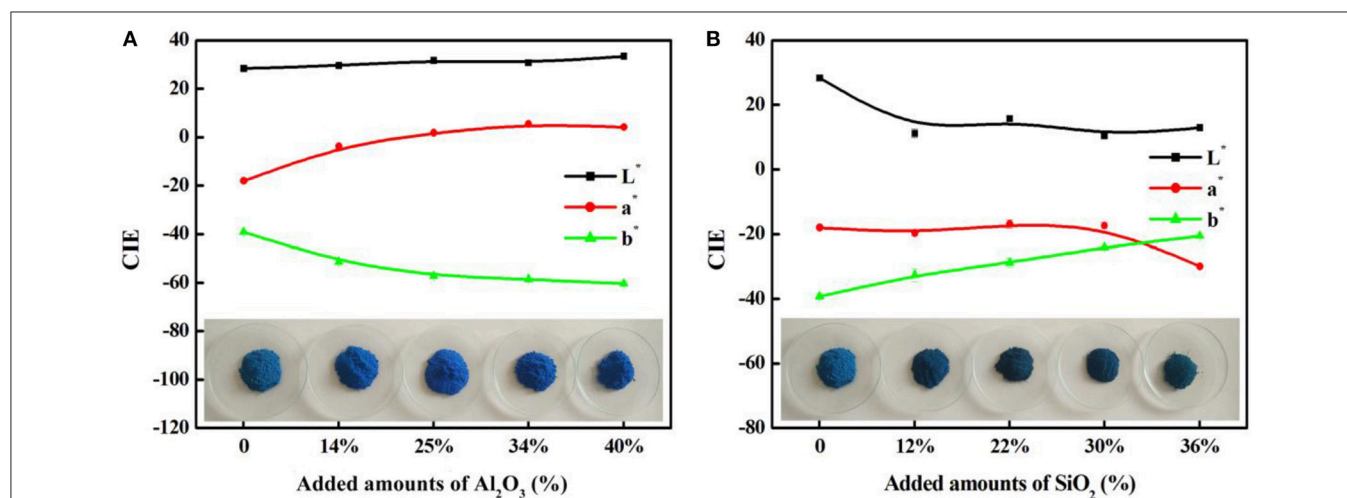
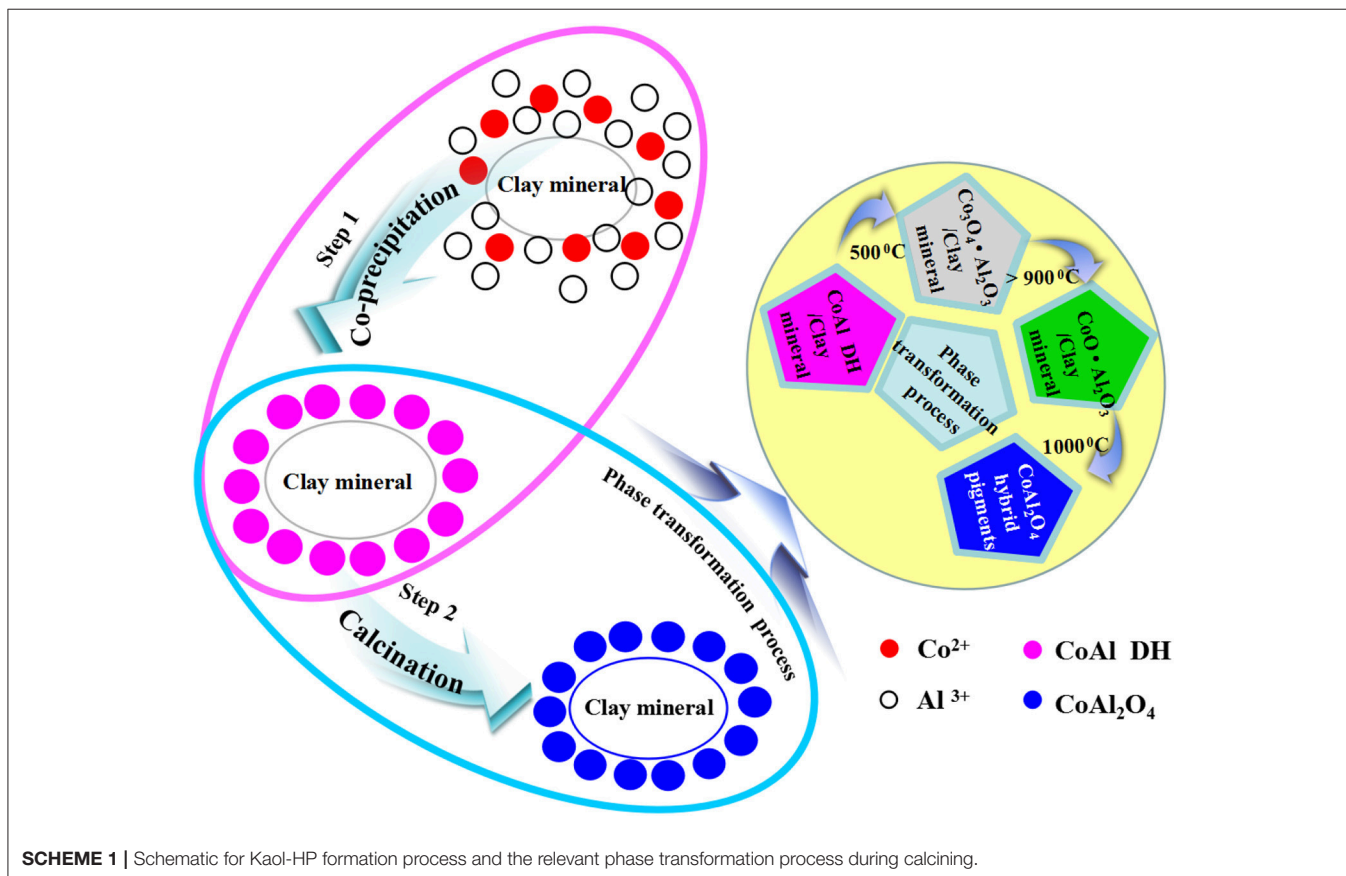
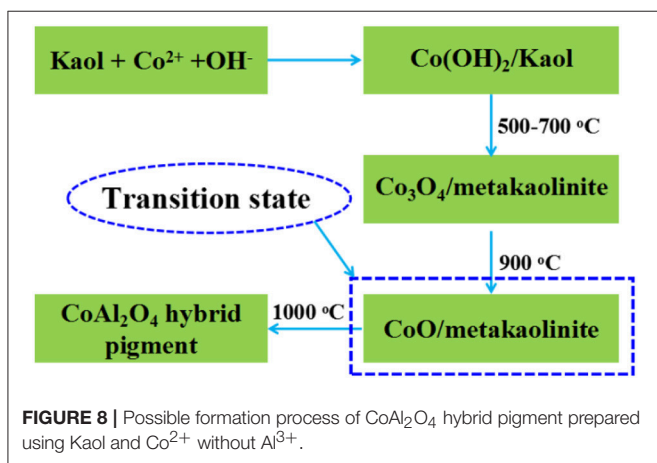


FIGURE 7 | The relationship between the CIE parameters of CoAl₂O₄ hybrid pigments prepared after incorporating of different added amounts of (A) Al₂O₃ and (B) SiO₂ without clay minerals, respectively.

Formation Mechanism of CoAl₂O₄ Hybrid Pigments

Based on the above results, the possible formation mechanism of CoAl₂O₄ hybrid pigments was proposed (Scheme 1). During the co-precipitation reaction, the Co²⁺ and Al³⁺ were firstly adsorbed on the surface of clay minerals due to the electrostatic interaction and ion exchange between metal ions and clay minerals, and then Co²⁺ and Al³⁺ were transformed into the hydroxides and deposited on the surface of clay mineral after

introducing of OH⁻. Due to the difference in the solubility constant of Al(OH)₃ and Co(OH)₂, Al³⁺ was firstly began to precipitate at lower pH, and then Co²⁺ was transformed into Co(OH)₂ at higher pH (Loganathan et al., 1977; He and Becker, 1997; Matjie et al., 2003; Akdemir et al., 2011). When the pH of reaction system was above 10, Co²⁺ almost precipitated completely, but Al(OH)₃ partially dissolved to form AlO₂⁻. As a result, the molar ratio of Co²⁺/Al³⁺ is <2. (Lavrenčič Štangar et al., 2003; Carta et al., 2005; Xu et al., 2008; Tielens et al., 2009; Kurajica et al., 2012). Therefore, CoAl DH was decomposed to form amorphous Co₃O₄ phase at around 400–500°C accompanied with the presence of highly amorphous Al₂O₃ once heating. With the increase in the calcining temperature (500–700°C), the amorphous Co₃O₄ was transformed into the spinel-type Co₃O₄ while Kaol was turned into metakaolinite (2SiO₂·Al₂O₃) (Yu et al., 2009; Duan et al., 2011), and Co₃O₄ was then progressively transformed into CoAl₂O₄ phase above 900°C, thus the content of spinel CoAl₂O₄ phase gradually increased with the vanishing of Co₃O₄ phase as the calcining temperature was above 1,000°C (Zayat and Levy, 2000; Duan et al., 2011; Álvarez-Docio et al., 2017; Zhang et al., 2018). In addition, metakaolinite was firstly transformed into spinel SiAl₂O₅ and amorphous SiO₂, and then the spinel SiAl₂O₅ changed into amorphous SiO₂ and low-order crystalline α-Al₂O₃ above 1,000°C (Chen et al., 2000; Ribeiro et al., 2005; Veselý et al., 2010; Wu et al., 2017). In fact, the thermal reduction of Co³⁺ to



Co²⁺ was simultaneous with the diffusion and reorganization of Co²⁺ and Al³⁺ ions derived from the precursor and clay minerals during this process.

It is well-known that the mass transfer process was the controlling rate step during CoAl₂O₄ preparation (Gabrovská et al., 2014). Therefore, the aluminosilicate clay minerals induced the anchoring of CoAl DH on their surface preventing from the free aggregations of CoAl DH, which could effectively decrease mass transfer resistance to reduce the time and calcining temperature for formation of spinel CoAl₂O₄. In addition, it was in favor of controlling the size and particle size distribution of CoAl₂O₄ nanoparticles during calcination process. What's more, Al³⁺ derived from aluminosilicate clay mineral also participated in the CoAl₂O₄ crystallization by the diffusion from substrate to compensate the aluminum loss during the co-precipitation reaction (Wang et al., 2006; Álvarez-Docio et al., 2017). Therefore, it may explain why the bright blue CoAl₂O₄ hybrid pigments could be obtained at 1,100°C for 2 h, but the traditional solid phase method for preparation of CoAl₂O₄ must be conducted at high temperature (>1,200°C) for a long time (Ji et al., 2000; Lorite et al., 2012). Especially, the hybrid pigments derived from the 1:1 style aluminosilicate clay minerals presented high CIE parameters. Due to the higher affinity of CoO to Al₂O₃ than SiO₂, and the CoO was easily arrived to the interphase of α -Al₂O₃ originating from aluminosilicate clay mineral to generate CoAl₂O₄ (Ahmed et al., 2012). For 2:1 style aluminosilicate clay minerals, the aluminosilicate clay minerals transformed into amorphous SiO₂ and α -Al₂O₃ at high temperature, and the content of SiO₂ is much higher than that of α -Al₂O₃. CoO might react with partially SiO₂ to form the CoSiO₃, which led to poor color properties of hybrid pigment. In order to prove above proposal, XRD patterns of Kaol-HP and Mt-HP are compared (Figure S9), it is clear that the CoSiO₃ (JCPD card no. 72-1508) occurs in Mt-HP accompanied with SiO₂ (JCPD card no. 86-0680), but they cannot be found in XRD pattern of Kaol-HP.

CONCLUSIONS

In summary, different aluminosilicate clay minerals were employed to prepare the CoAl₂O₄ hybrid pigment with different

color properties. It was found that the more content of Al₂O₃, the better color properties of hybrid pigment (higher lightness and blue), suggesting that the rich-aluminum silicate mineral was appropriate for preparation of bright blue cobalt blue pigment. The aluminosilicate clay mineral was served as a carrier to load CoAl₂O₄ nanoparticles, preventing from the aggregation and controlling the size of CoAl₂O₄ nanoparticles during calcining process. What's more, it was an ideal natural aluminum sources to compensate the aluminum loss due to the dissolution of Al(OH)₃ at alkaline medium during preparation of precursor, keeping an optimum molar ratio of Co²⁺/Al³⁺ for formation of spinel CoAl₂O₄ pigments during high-temperature crystallization. Therefore, this study may provide a feasible strategy not only to develop low-cost and bright blue cobalt blue pigments, but also to control the color properties of cobalt blue by adjusting the types of clay minerals to meet the personalized demand in the practice application.

AUTHOR CONTRIBUTIONS

AZ and XW contribute to the experiment process, data analysis, and paper preparation. BM and AW are mainly responsible for the design of experiment, data analysis and paper revision. LW contributes to the samples characterization.

ACKNOWLEDGMENTS

The authors are grateful for financial support of Regional Key Project of the Science and Technology Service (STS) of the Chinese Academy of Sciences [(2016) No. 70], the Youth Innovation Promotion Association of CAS (2017458), Major Science and Technology Projects of Lanzhou (2017-2-3), the Funds for Creative Research Groups of Gansu, China (No. 17JR5RA306) and the fifth 333 project of Jiangsu Province of China (No. BRA2017259 and BRA2016244).

SUPPLEMENTARY MATERIAL

The Supplementary Material for this article can be found online at: <https://www.frontiersin.org/articles/10.3389/fchem.2018.00125/full#supplementary-material>

REFERENCES

- Abaide, E. R., Anchieta, C. G., Foletto, V. S., Reinehr, B., Nunes, L. F., Kuhn, R. C., et al. (2015). Production of copper and cobalt aluminate spinels and their application as supports for inulinase immobilization. *Mat. Res.* 18, 1062–1069. doi: 10.1590/1516-1439.031415
- Ahmed, N. A., Abdel-Fatah, H. T. M., and Youssef, E. A. (2012). Corrosion studies on tailored Zn-Co aluminate/kaolin core-shell pigments in alkyd based paints. *Prog. Org. Coat.* 73, 76–87. doi: 10.1016/j.porgcoat.2011.09.003
- Akdemir, S., Ozel, E., and Suvaci, E. (2011). Solubility of blue CoAl₂O₄ ceramic pigments in water and diethylene glycol media. *Ceram. Int.* 37, 863–870. doi: 10.1016/j.ceramint.2010.10.031
- Álvarez-Docio, C. M., Reinoso, J. J., Del Campo, A., and Fernández, J. F. (2017). 2D particles forming a nanostructured shell: a step forward cool NIR reflectivity for CoAl₂O₄ pigments. *Dyes Pigments* 137, 1–11. doi: 10.1016/j.dyepig.2016.09.061
- Armijo, J. S. (1969). The kinetics and mechanism of solid-state spinel formation-review and critique. *Oxid. Met.* 1, 171–198. doi: 10.1007/BF00603514
- Carta, G., Casarin, M., Habra, N., and Zanella, P. (2005). MOCVD deposition of CoAl₂O₄ films. *Electrochim. Acta* 50, 4592–4599. doi: 10.1016/j.electacta.2004.10.094
- Cava, S., Tebcherani, S. M., Pianaro, S. A., Paskocimas, C. A., Longo, E., and Varela, J. A. (2006). Structural and spectroscopic analysis of γ -Al₂O₃ to α -Al₂O₃-CoAl₂O₄ phase transition. *Mater. chem. phys.* 97, 102–108. doi: 10.1016/j.matchemphys.2005.07.057
- Chafi, M. S., Ghasemi, B., and Arabi, A. M. (2017). Solution combustion synthesis (SCS) of chrome alumina as a high temperature pink pigment. *Int. J. Appl. Ceram. Tec.* 15, 203–209. doi: 10.1111/ijac.12770
- Chapskaya, A. Y., Radishevskaya, N. I., Kasatskii, N. G., Lepakova, O. K., Naiborodenko, Y. S., and Vereshchagin, V. V. (2005). The effect of composition

- and synthesis conditions on the structure of cobalt-bearing pigments of the spinel type. *Glass Ceram.* 62, 388–390. doi: 10.1007/s10717-006-0016-x
- Chen, C. Y., Lan, C. S., and Tuan, W. H. (2000). Microstructural evolution of mullite during the sintering of kaolin powder compacts. *Ceram. Int.* 26, 715–720. doi: 10.1016/S0272-8842(00)00009-2
- Cho, W. S., and Kakihana, M. (1999). Crystallization of ceramic pigment CoAl₂O₄ nanocrystals from Co-Al metal organic precursor. *J. Alloys Compd.* 287, 87–90. doi: 10.1016/S0925-8388(99)00059-6
- De Souza, L. K. C., Zamian, J. R., Da Rocha Filho, G. N., Soledadeb, L. E. B., Dos Santos, I. M. G., Souza, A. G., et al. (2009). Blue pigments based on Co_xZn_{1-x}Al₂O₄ spinels synthesized by the polymeric precursor method. *Dyes Pigments* 81, 187–192. doi: 10.1016/j.dyepig.2008.09.017
- Duan, X., Pan, M., Yu, F., and Yuan, D. R. (2011). Synthesis, structure and optical properties of CoAl₂O₄ spinel nanocrystals. *J. Alloy. Compd.* 509, 1079–1083. doi: 10.1016/j.jallcom.2010.09.199
- Ezzatahmedi, N., Ayoko, G. A., Millar, G. J., Speight, R., Yan, C., Li, J. H., et al. (2017). Clay-supported nanoscale zero-valent iron composite materials for the remediation of contaminated aqueous solutions: a review. *Chem. Eng. J.* 312, 336–350. doi: 10.1016/j.cej.2016.11.154
- Gabrovsk, M. V., Crisan, D., Stanica, N., and Kardjiev, R. (2014). Co-Al layered double hydroxides as precursors of ceramic pigment CoAl₂O₄. Part I: phase composition. *Rev. Roum. Chim.* 59, 445–450.
- Gholizadeh, A., and Malekzadeh, A. (2017). Structural and redox features of La_{0.7}Bi_{0.3}Mn_{1-x}Co_xO₃ nanoperovskites for ethane combustion and CO oxidation. *Int. J. Appl. Ceram. Tec.* 14, 404–412. doi: 10.1111/ijac.12650
- He, T., and Becker, K. D. (1997). An optical *in-situ* study of a reacting spinel crystal. *Solid State Ionics* 101, 337–342. doi: 10.1016/S0167-2738(97)84050-7
- He, Y., Cao, Y., Liao, H. L., and Wang, J. A. (2017). Preparation of porous cobalt aluminate and its chromogenic mechanism. *Powder Technol.* 324, 95–101. doi: 10.1016/j.powtec.2017.08.056
- Intachai, S., Suppasso, C., Klinrsisuk, S., Khaorapapong, N., and Ogawa, M. (2017). The possible doping of Al³⁺ and F⁻ modification onto GdS in montmorillonite. *Colloid Surf. A Physicochem. Eng. Asp.* 522, 133–139. doi: 10.1016/j.colsurfa.2017.02.044
- Jafari, M., and Hassanzadeh-Tabrizi, S. A. (2014). Preparation of CoAl₂O₄ nanoblu pigment by polyacrylamide gel method. *Powder Technol.* 266, 236–239. doi: 10.1016/j.powtec.2014.06.018
- Ji, L., Lin, J., and Zeng, H. C. (2000). Metal-support interactions in Co/Al₂O₃ catalysts: a comparative study on reactivity of support. *J. Phys. Chem. B* 104, 1783–1790. doi: 10.1021/jp9934001
- Juneja, A., Hegde, A., Lee, F. H., and Yeo, C. H. (2010). Centrifuge modelling of tunnel face reinforcement using forepoling. *Tunn. Undergr. Space Tech.* 25, 377–381. doi: 10.1016/j.tust.2010.01.013
- Kamaraj, A., and Vasudevan, S. (2016). Facile one-pot electrosynthesis of Al(OH)₃-kinetics and equilibrium modeling for adsorption of 2,4,5-trichlorophenoxyacetic acid from aqueous solution. *New J. Chem.* 40, 2249–2258. doi: 10.1039/C5NJ02407B
- Khattab, R. M., Sadek, H. E. H., and Gaber, A. A. (2017). Synthesis of Co_xMg_{1-x}Al₂O₄ nanospinel pigments by microwave combustion method. *Ceram. Int.* 43, 234–243. doi: 10.1016/j.ceramint.2016.09.144
- Kim, J. H., Son, B. R., Yoon, D. H., Hwang, K. T., Noh, H. G., Cho, W. S., et al. (2012). Characterization of blue CoAl₂O₄ nano-pigment synthesized by ultrasonic hydrothermal method. *Ceram. Int.* 38, 5707–5712. doi: 10.1016/j.ceramint.2012.04.015
- Konduri, M. K. R., and Fatehi, P. (2017). Dispersion of kaolin particles with carboxymethylated xylan. *Appl. Clay Sci.* 137, 183–191. doi: 10.1016/j.clay.2016.12.027
- Kurajica, S., Popović, J., Tkalcic, E., Gržeta, B., and Mandić, V. (2012). The effect of annealing temperature on the structure and optical properties of sol-gel derived nanocrystalline cobalt aluminate spinel. *Mater. Chem. Phys.* 135, 587–593. doi: 10.1016/j.matchemphys.2012.05.030
- Lavrenčić Štangar, U., Orel, B., and Krajnc, M. (2003). Preparation and spectroscopic characterization of blue CoAl₂O₄ coatings. *J. Sol Gel Sci. Technol.* 26, 771–775. doi: 10.1023/A:1020770810027
- Liang, H., Wang, Z. Q., Liao, L. M., Chen, L., Li, Z., and Feng, J. (2017). High performance photocatalysts: montmorillonite supported-nano TiO₂ composites. *Optik* 136, 44–51. doi: 10.1016/j.ijleo.2017.02.018
- Llusar, M., Forés, A., Badenes, J. A., Calbo, J., Tena, M. A., and Monrós, G. (2001). Colour analysis of some cobalt-based blue pigments. *J. Eur. Ceram. Soc.* 21, 1121–1130. doi: 10.1016/S0955-2219(00)00295-8
- Loganathan, P., Burau, R. G., and Fuerstenau, D. W. (1977). Influence of pH on the sorption of Co²⁺, Zn²⁺ and Ca²⁺ by a hydrous manganese oxide. *Soil Sci. Soc. Am. J.* 41, 57–62. doi: 10.2136/sssaj1977.03615995004100010020x
- Lorite, I., Campo, A., Romero, J. J., and Fernández, J. F. (2012). Isolated nanoparticle Raman spectroscopy. *J. Raman Spectrosc.* 43, 889–894. doi: 10.1002/jrs.3112
- Mahé, M., Heintz, J., Rödel, J., and Reynnders, P. (2008). Cracking of titania nanocrystalline coatings. *J. Eur. Ceram. Soc.* 28, 2003–2010. doi: 10.1016/j.jeurceramsoc.2008.02.002
- Matjie, R. H., Mdleleni, M. M., and Scurrall, M. S. (2003). Extraction of cobalt (II) from an ammonium nitrate-containing leach liquor by an ammonium salt of di (2-ethylhexyl) phosphoric acid. *Miner. Eng.* 16, 1013–1017. doi: 10.1016/S0892-6875(03)00265-6
- Meng, K., Gao, S., Wu, L., Wang, G., Liu, X., Chen, G., et al. (2016). Two-dimensional organic-inorganic hybrid perovskite photonic films. *Nano Lett.* 16, 4166–4173. doi: 10.1021/acs.nanolett.6b01046
- Merino, M. C. G., Estrella, A. L., Rodriguez, M. E., and Vázquez, P. (2015). Combustion syntheses of CoAl₂O₄ powders using different fuels. *Prog. Mater. Sci.* 8, 519–525. doi: 10.1016/j.mspro.2015.04.104
- Mindru, I., Marinescu, G., Gingasu, D., Patron, L., Ghica, C., and Giurginca, M. (2010). Blue CoAl₂O₄ spinel via complexation method. *Mater. Chem. Phys.* 122, 491–497. doi: 10.1016/j.matchemphys.2010.03.032
- Mishra, A., Mehta, A., Sharma, M., and Basu, S. (2017). Enhanced heterogeneous photodegradation of VOC and dye using microwave synthesized TiO₂/Clay nanocomposites: a comparison study of different type of clays. *J. Alloy. Compd.* 694, 574–580. doi: 10.1016/j.jallcom.2016.10.036
- Mousavand, T., Takami, S., Umetsu, M., Ohara, S., and Adschiri, T. (2006). Supercritical hydrothermal synthesis of organic-inorganic hybrid nanoparticles. *J. Mater. Sci.* 41, 1445–1448. doi: 10.1007/s10853-006-7458-y
- Mu, B., and Wang, A. Q. (2015). One-pot fabrication of multifunctional superparamagnetic attapulgite/Fe₃O₄/polyaniline nanocomposites served as adsorbent and catalyst support. *J. Mater. Chem. A* 3, 281–289. doi: 10.1039/C4TA05367B
- Mu, B., Wang, Q., and Wang, A. Q. (2015). Effect of different clay minerals and calcination temperature on the morphology and color of clay/CoAl₂O₄ hybrid pigments. *RSC Adv.* 5, 102674–102681. doi: 10.1039/C5RA19955G
- Ouahdi, N., Guillemet, S., Demai, J. J., Durand, B., Er Rakho, L., Moussa, R., et al. (2005). Investigation of the reactivity of AlCl₃ and CoCl₂ toward molten alkali-metal nitrates in order to synthesize CoAl₂O₄. *Mater. Lett.* 59, 334–340. doi: 10.1016/j.matlet.2004.10.013
- Panda, A. K., Mishra, B. G., Mishra, D. K., and Singha, R. K. (2010). Effect of sulphuric acid treatment on the physico-chemical characteristics of kaolin clay. *Colloid Surf. A Physicochem. Eng. Asp.* 363, 98–104. doi: 10.1016/j.colsurfa.2010.04.022
- Philip, A., Lihavainen, J., Keinänen, M., and Pakkanen, T. T. (2017). Gold nanoparticle decorated halloysite nanotubes-selective catalysts for benzyl alcohol oxidation. *Appl. Clay Sci.* 143, 80–88. doi: 10.1016/j.clay.2017.03.015
- Rani, G. (2017). Annealing effect on the structural, optical and thermoluminescent properties of ZnAl₂O₄:Cr³⁺. *Powder Technol.* 312, 354–359. doi: 10.1016/j.powtec.2017.02.040
- Ren, Z., Botu, V., Wang, S., Meng, Y., Song, W., Guo, Y., et al. (2014). Monolithically integrated spinel M_xCo_{3-x}O₄ (M=Co, Ni, Zn) nanoarray catalysts: scalable synthesis and cation manipulation for tunable low-temperature CH₄ and CO oxidation. *Angew. Chem. Int. Edit.* 53, 7223–7227. doi: 10.1002/anie.201403461
- Ribeiro, M. J., Tulyagavov, D. U., Ferreira, J. M., and Labrincha, J. A. (2005). High temperature mullite dissolution in ceramic bodies derived from Al-rich sludge. *J. Eur. Ceram. Soc.* 25, 703–710. doi: 10.1016/j.jeurceramsoc.2004.03.028
- Ryu, Y. C., Kim, T. G., Seo, G., Park, J. H., Suh, C. S., Park, S., et al. (2008). Effect of substrate on the phase transformation of TiO₂ in pearlescent pigment. *J. Ind. Eng. Chem.* 14, 213–218. doi: 10.1016/j.jiec.2007.11.004
- Saikia, B. J., and Parthasarathy, G. (2010). Fourier transform infrared spectroscopic characterization of kaolinite from Assam and Meghalaya, Northeastern India. *J. Mod. Phys.* 1, 206–210. doi: 10.4236/jmp.2010.14031

- Salavati-Niasari, M., Khansari, A., and Davar, F. (2009). Synthesis and characterization of Co₃O₄ nanoparticles by thermal treatment process. *J. Clust. Sci.* 362, 4937–4942. doi: 10.1016/j.ica.2009.07.023
- Sale, S. (2015). Relationship between gel rheology and specific surface area of nano-sized CoAl₂O₄ powder manufactured by autoignition technique. *Mater. Lett.* 139, 498–500. doi: 10.1016/j.matlet.2014.10.118
- Sedghi, A., Alimohammadi, M., and Zadeh, M. C. (2014). Structure and properties of Co_xZn_{1-x}Al₂O₄ nano-pigments fabricated by gel combustion method. *Ceram. Silikáty* 58, 145–150.
- Soeimani-Gorgania, A., Ghaharib, M., and Peymannia, M. (2015). *In-situ* production of nano-CoAl₂O₄ on a ceramic surface by ink-jet printing. *J. Eur. Ceram. Soc.* 35, 779–786. doi: 10.1016/j.jeurceramsoc.2014.08.047
- Tang, W. X., Ren, Z., Lu, X. X., Wang, S. B., Guo, Y. B., Hoang, S., et al. (2017). Scalable integration of highly uniform Mn_xCo_{3-x}O₄ nano-sheet array onto ceramic monolithic substrates for low temperature propane oxidation. *ChemCatChem* 9, 4112–4119. doi: 10.1002/cctc.201700795
- Tang, Y., Wu, C., Song, Y., Zheng, Y., and Zhao, K. (2018). Effects of colouration mechanism and stability of CoAl₂O₄ ceramic pigments sintered on substrates. *Ceram. Int.* 44, 1019–1025. doi: 10.1016/j.ceramint.2017.10.038
- Tian, G. Y., Wang, W. B., Wang, D. D., Wang, Q., and Wang, A. Q. (2017). Novel environment friendly inorganic red pigments based on attapulgite. *Powder Technol.* 315, 60–67. doi: 10.1016/j.powtec.2017.03.044
- Tielsens, F., Calatayud, M., Franco, R., Recio, J. M., Pérez-Ramírez, J., and Minot, C. (2009). Theoretical investigation of the inversion parameter in Co_{3-s}Al_sO₄ (s = 0–3) spinel structures. *Solid State Ionics* 180, 1011–1016. doi: 10.1016/j.ssi.2009.03.023
- Tirsoaga, A., Visinescu, D., Jurca, B., Ianculescu, A., and Carp, O. (2011). Eco-friendly combustion-based synthesis of metal aluminates MAl₂O₄ (M = Ni, Co). *J. Nanopart. Res.* 13, 6397–6408. doi: 10.1007/s11051-011-0392-1
- Todorova, N., Giannakopoulou, T., Karapati, S., Petridis, D., Vaimakis, T., and Trapalis, C. (2014). Composite TiO₂/clays materials for photocatalytic NO_x oxidation. *Appl. Surf. Sci.* 319, 113–120. doi: 10.1016/j.apsusc.2014.07.020
- Torkian, L., Daghighi, M., and Boorboor, Z. (2013). Simple and efficient route for synthesis of spinel nanopigments. *J. Chem.* 2013, 1–6. doi: 10.1155/2013/694531
- Vesely, D., Kalendova, A., and Kalenda, P. A. (2010). Study of diatomite and calcined kaoline properties in anticorrosion protective coatings. *Prog. Org. Coat.* 68, 173–179. doi: 10.1016/j.porgcoat.2010.02.007
- Wang, C., Liu, S. M., Liu, L. H., and Bai, X. (2006). Synthesis of cobalt-aluminate spinels via glycine chelated precursors. *Mater. Chem. Phys.* 96, 361–370. doi: 10.1016/j.matchemphys.2005.07.066
- Wang, G. F., Wang, S., Sun, W., Sun, Z. M., and Zheng, S. L. (2016). Synthesis of a novel illite@carbon nanocomposite adsorbent for removal of Cr (VI) from wastewater. *J. Environ. Sci.* 57, 62–71. doi: 10.1016/j.jes.2016.10.017
- Wang, R. J., Jiang, G. H., Ding, Y. W., Wang, Y., Sun, X. K., Wang, X. H., et al. (2011). Photocatalytic activity of heterostructures based on TiO₂ and halloysite nanotubes. *Appl. Mater. Inter.* 3, 4154–4158. doi: 10.1021/am201020q
- Wu, J. F., Hu, C., Xu, X. H., and Zhang, Y. F. (2017). Preparation and performance study of Mullite/Al₂O₃ composite ceramics for solar thermal transmission pipeline. *Int. J. Appl. Ceram. Tec.* 13, 1017–1023. doi: 10.1111/ijac.12584
- Xu, X. H., Li, J. W., Wu, J. F., Tang, Z. H., Chen, L. L., Li, Y., et al. (2017). Preparation and thermal shock resistance of corundum-mullite composite ceramics from andalusite. *Ceram. Int.* 43, 1762–1767. doi: 10.1016/j.ceramint.2016.10.116
- Xu, X. H., Qin, X. F., Jiang, F. X., Li, X. L., Chen, Y., and Gehring, G. A. (2008). The dopant concentration and annealing temperature dependence of ferromagnetism in Co-doped ZnO thin films. *Appl. Surf. Sci.* 254, 4956–4960. doi: 10.1016/j.apsusc.2008.01.164
- Yeo, C. H. (2011). *Stability and Collapse Mechanisms of Unreinforced and Forepole-Reinforced Tunnel Headings*. Ph.D. thesis, National University of Singapore, Singapore.
- Yoneda, M., Gotoh, K., Nakanishi, M., Fujii, T., and Nomura, T. (2016). Influence of aluminum source on the color tone of cobalt blue pigment. *Powder Technol.* 323, 574–580. doi: 10.1016/j.powtec.2016.06.021
- Yu, F., Yang, J., Ma, J., Du, J., and Zhou, Y. Q. (2009). Preparation of nanosized CoAl₂O₄ powders by sol-gel and sol-gel-hydrothermal methods. *J. Alloy. Compd.* 468, 443–446. doi: 10.1016/j.jallcom.2008.01.018
- Yuan, L., Ma, B. Y., Zhu, Q., Zhang, X. D., Zhang, H., and Yu, J. K. (2017). Preparation and properties of mullite-bonded porous fibrous mullite ceramics by an epoxy resin gel-casting process. *Ceram. Int.* 43, 5478–5483. doi: 10.1016/j.ceramint.2017.01.062
- Zayat, M., and Levy, D. (2000). Blue CoAl₂O₄ particles prepared by the sol-gel and citrate-gel methods. *Chem. Mater.* 12, 2763–2769. doi: 10.1021/cm001061z
- Zhang, A. J., Mu, B., Li, H. M., An, X. C., and Wang, A. Q. (2018). Cobalt blue hybrid pigment doped with magnesium derived from sepiolite. *Appl. Clay Sci.* 157, 111–120. doi: 10.1016/j.clay.2018.02.032
- Zhang, A. J., Mu, B., and Wang, A. Q. (2017). Bright blue halloysite/CoAl₂O₄ hybrid pigments: preparation, characterization and application in water-based painting. *Dyes Pigments* 139, 473–481. doi: 10.1016/j.dyepig.2016.12.055
- Zhang, Y., Wang, W. B., Mu, B., Wang, Q., and Wang, A. Q. (2015). Effect of grinding time on fabricating a stable methylene blue/palygorskite hybrid nanocomposite. *Powder Technol.* 280, 173–179. doi: 10.1016/j.powtec.2015.04.046
- Zheng, Q. M., Liu, Q. F., Shen, Q., Wu, Z. G., and Zhang, Y. M. (2011). The mineralogical characteristics and genesis of the dickite in Taiyuan formation in Southeastern Shanxi. *Proc. Eng.* 26, 898–901. doi: 10.1016/j.proeng.2011.11.2253
- Zhong, Z. Y., Mastai, Y., Koltypin, Y., Zhao, Y. M., and Gedanken, A. (1999). Sonochemical coating of nanosized nickel on alumina microspheres and the interaction between the nickel and nickel oxide with the substrate. *Chem. Mater.* 11, 2350–2359. doi: 10.1021/cm981005m
- Zou, J., and Zheng, W. (2016). TiO₂@CoTiO₃ complex green pigments with low cobalt content and tunable color properties. *Ceram. Int.* 42, 8198–8205. doi: 10.1016/j.ceramint.2016.02.029

Conflict of Interest Statement: The authors declare that the research was conducted in the absence of any commercial or financial relationships that could be construed as a potential conflict of interest.

The reviewer SW and handling Editor declared their shared affiliation.

Copyright © 2018 Zhang, Mu, Wang, Wen and Wang. This is an open-access article distributed under the terms of the Creative Commons Attribution License (CC BY). The use, distribution or reproduction in other forums is permitted, provided the original author(s) and the copyright owner are credited and that the original publication in this journal is cited, in accordance with accepted academic practice. No use, distribution or reproduction is permitted which does not comply with these terms.